

# Edge-enhanced imaging with polyvinyl alcohol/acrylamide photopolymer gratings

Andrés Márquez, Cristian Neipp, and Augusto Beléndez

*Departamento de Física, Ingeniería de Sistemas y Teoría de la Señal, Universidad de Alicante, Apartado 99, E-03080 Alicante, Spain*

Sergi Gallego, Manuel Ortuño, and Inmaculada Pascual

*Departamento Interuniversitario de Óptica, Universidad de Alicante, Apartado 99, E-03080 Alicante, Spain*

Received February 25, 2003

We demonstrate edge-enhanced imaging produced by volume phase gratings recorded on a polyvinyl alcohol/acrylamide photopolymer. Bragg diffraction, exhibited by volume gratings, modifies the impulse response of the imaging system, facilitating spatial filtering operations with no need for a physical Fourier plane. We demonstrate that Kogelnik's coupled-wave theory can be used to calculate the transfer function for the transmitted and the diffracted orders. The experimental and simulated results agree, and they demonstrate the feasibility of our proposal. © 2003 Optical Society of America

OCIS codes: 050.0050, 090.7330, 100.1160, 160.5470.

In recent years, novel applications for diffraction gratings have been suggested by those working with acousto-optic light modulators (AOLMs): Gratings generated in AOLMs in the Bragg regime are useful for image processing operations in imaging systems.<sup>1-4</sup> Bragg diffraction offers unique properties such as wavelength and angular selectivity<sup>5</sup>; the latter is responsible for the image processing applications reported with AOLMs. However, when programmability of AOLMs was not needed, a wide variety of materials and technologies<sup>6</sup> become available. Among them, holography offers a natural and inexpensive way to register high-quality volume gratings.<sup>5</sup> In the 1970s Case<sup>7</sup> showed edge enhancement produced in imaging systems by holographically recorded dichromated gelatin gratings. Previously, Peri and Friesem<sup>8</sup> reported the application of volume gratings to polymethyl cyanoacrylate for image restoration. Lately some different holographic materials, especially photopolymers, have received great attention as promising media for write-once-read-many holographic data storage applications.<sup>9</sup> We are especially interested in polyvinyl alcohol/acrylamide (PVA) compounds that combine good optical properties, ease of fabrication, and self-development capability.<sup>10,11</sup> In this Letter we focus on the application of photopolymers to image processing in imaging systems by Bragg diffraction. In particular, we demonstrate image edge enhancement produced by a PVA/acrylamide volume phase grating. In addition, we show that we can apply Kogelnik's<sup>12</sup> close-form expressions to describe the performance of volume gratings in image processing.

Image processing operations by Bragg diffraction are based on the angular selectivity presented by the zero and the first diffracted orders of volume gratings. Whereas the zero (or transmitted) order behaves as a spatial high-pass filter, the first (or diffracted) order has the characteristics of a low-pass filter. These Bragg diffraction effects in

AOLMs have been described by use of the spatial-frequency transfer function formalism.<sup>4</sup> Next, we show that the classic closed-form expressions from Kogelnik's theory<sup>12</sup> provide a direct way to obtain accurate spatial-frequency transfer functions for holographic gratings. According to Kogelnik's theory, for a volume phase unslanted transmission grating the expressions for the transmitted,  $R$ , and the diffracted,  $S$ , wave amplitudes after the waves pass through the hologram are

$$R = \exp(-j\xi) (\cos\sqrt{v^2 + \xi^2} + j\xi \operatorname{sinc}\sqrt{v^2 + \xi^2}), \quad (1a)$$

$$S = \exp(-j\xi) (-jv)\operatorname{sinc}\sqrt{v^2 + \xi^2}, \quad (1b)$$

where  $\operatorname{sinc}(x) = \sin(x)/x$ ,

$$v = \frac{\pi \Delta n d}{\lambda_0 \cos \theta_r'},$$

$$\xi = \frac{\pi d}{\Lambda \cos \theta_r'} \left( |\sin \theta_r'| - \frac{\lambda_0}{2n_0 \Lambda} \right), \quad (2)$$

$n_0$  and  $\Delta n$  are, respectively, the average and the modulation of the refractive index,  $d$  is the thickness of the medium,  $\Lambda$  is the period of the grating,  $\lambda_0$  is the wavelength of reconstruction in air, and  $\theta_r'$  is the angle of reconstruction in the recording medium related by Snell's law to angle of reconstruction in air  $\theta_r$ . Bragg angle  $\theta_{\text{Bragg}}'$  inside the material is given by  $\sin \theta_{\text{Bragg}}' = \lambda_0 / 2n_0 \Lambda$ ; thus  $\xi$  expresses deviation from the Bragg condition. Parameter  $v$  expresses the amplitude of the phase modulation recorded in the volume grating.

Wave amplitudes  $R$  and  $S$  given by Eqs. (1) depend on angle  $\theta_r$  of the incident beam with respect to the normal of the hologram. According to Fig. 1, let us consider  $\theta_o$  and  $\psi$ , respectively, the angles of

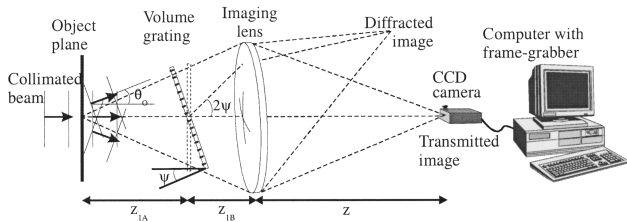


Fig. 1. Setup for image formation with a holographic grating. We show the deviation of the transmitted and the diffracted images caused by the grating.

the plane-wave spectrum of an input object and the orientation of the grating with respect to the optical axis in a specific optical system. Thus angle  $\theta_r$  is given by  $\theta_r = \theta_o - \psi$ , and angular responses  $R$  and  $S$  of the grating modify the spectrum of plane waves propagating from the object. Similarly, Eq. (1) can be expressed as a function of angular frequency  $p$  (in radians per meter), given by  $p = 2\pi \sin \theta_o / \lambda_0$ , to produce angular frequency transfer functions  $H_0(p)$  and  $H_1(p)$  for the zero and the first diffracted orders, respectively. Interesting properties arise when the grating is oriented at  $\psi = \theta_{\text{Bragg}}$ , where  $\theta_{\text{Bragg}}$  is the Bragg angle in air. To compare Kogelnik's expressions with those for AOLMs we proceed with some simplifications. In the paraxial approximation, i.e., when angle of incidence  $\theta_r$  is small, Eqs. (2) become

$$\xi = \frac{Q\Lambda}{4\pi} p, \quad v = \frac{\pi\Delta nd}{\lambda_0}, \quad (3)$$

where  $Q = (2\pi\lambda_0 d) / n_0 \Lambda^2$  is the Klein-Cook parameter that expresses the magnitude of volume effects.<sup>5</sup> Substitution of the expressions in Eqs. (3) into Eqs. (1) results in the angular frequency transfer functions

$$H_0(p) = \exp\left(-j \frac{Q\Lambda}{4\pi} p\right) \left( \cos\left[\left(\frac{Q\Lambda}{4\pi} p\right) + \left(\frac{\pi\Delta nd}{\lambda_0}\right)^2\right]^{1/2} + j \left(\frac{Q\Lambda}{4\pi} p\right) \text{sinc}\left[\left[\left(\frac{Q\Lambda}{4\pi} p\right)^2 + \left(\frac{\pi\Delta nd}{\lambda_0}\right)^2\right]^{1/2}\right] \right), \quad (4a)$$

$$H_1(p) = \exp\left(-j \frac{Q\Lambda}{4\pi} p\right) \left(-j \frac{\pi\Delta nd}{\lambda_0}\right) \times \text{sinc}\left[\left[\left(\frac{Q\Lambda}{4\pi} p\right)^2 + \left(\frac{\pi\Delta nd}{\lambda_0}\right)^2\right]^{1/2}\right]. \quad (4b)$$

These expressions of Kogelnik's are totally coincident with previous expressions obtained with AOLMs by other approaches.<sup>2</sup> We can see that the exponential factor is linear in  $p$ , thus giving rise to a shift in the propagation of the incident plane waves. This term represents the shift produced by refraction in a plane-parallel plate. The remaining terms characterize the interaction between the transmitted and the diffracted waves inside the hologram. For small angles,  $\xi^2 \ll v^2$ , a direct interpretation of the effects of this interaction can be given. Davis and Nowak<sup>3</sup> showed that, in this approximation, by changing the amplitude of the sound wave in the AOLM, which is equivalent to a change in  $v$ , it is possible to select

the edges that will be enhanced and the degree of enhancement. When  $v = \pi/2$ , transfer function  $H_0(p)$  becomes a derivative filter. In general,  $H_0(p)$  behaves as a high-pass filter and  $H_1(p)$  has the characteristics of a low-pass filter.

In the experiments a He-Ne laser beam ( $\lambda = 633 \text{ nm}$ ) is spatially filtered, expanded, and collimated. The distances in the setup (Fig. 1) are  $z_{1A} = 12 \text{ cm}$ ,  $z_{1B} = 8 \text{ cm}$ , and  $z_2 = 59 \text{ cm}$ , the lens has a focal length  $f' = 15 \text{ cm}$  and a clear-aperture diameter  $\phi = 7.5 \text{ cm}$ , and the magnification of the system is  $3\times$ . We capture the transmitted (zero-order) image by using a Hamamatsu C5403 CCD camera and a Matrox Meteor frame grabber connected to a personal computer.

We used an unslanted phase grating recorded on a PVA/acrylamide photopolymer (preparation and composition details are given in Ref. 11) exposed to the green line (514 nm) of an argon laser with a symmetrical mount. The two beams form an angle of  $16.8^\circ$  with respect to the normal of the plate and generate an interference pattern of 1.5-cm diameter with a spatial frequency of 1125 lines/mm. In Fig. 2 we show the angular response (in intensity) of the transmitted order as a function of reconstruction angle  $\theta_r$  for a He-Ne laser beam. We see that the Bragg angle is  $20.8^\circ$  with a diffraction efficiency of 93%, close to the theoretical maximum of 100%. Circles represent experimental measurements, whereas the continuous curve corresponds to the theoretical fit from Kogelnik's theory with values  $n_0 = 1.50$ ,  $\Delta n = 0.003$ ,  $d = 88 \mu\text{m}$ , and a low absorption constant  $\alpha = 0.00092 \mu\text{m}^{-1}$ . The Klein-Cook parameter for the photopolymer grating used in the study reported here is  $Q \approx 300$ ; thus the grating is clearly in the Bragg regime. From Fig. 2 we can see that, if the notch in the angular response is centered at optical axis  $\psi = \theta_{\text{Bragg}}$ , the angular response for the transmitted order will have the shape of a high-pass spatial filter. Low spatial frequencies of the object are then diffracted into the first order and blocked from the zero order.

In Fig. 3 we show some simulated results to compare with the experiment. We simulate the spatial filtering operation performed by zero-order transfer function  $H_0(p)$  associated with the angular response

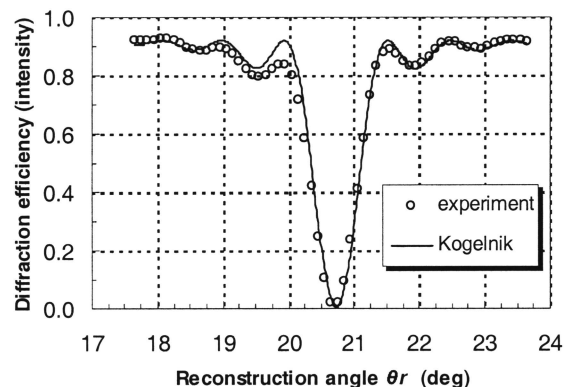


Fig. 2. Angular response in intensity, from experiment and from Kogelnik's fit, for the photopolymer grating used. We used a He-Ne laser beam ( $\lambda = 633 \text{ nm}$ ). Bragg angle,  $20.8^\circ$ ;  $Q \approx 300$ .

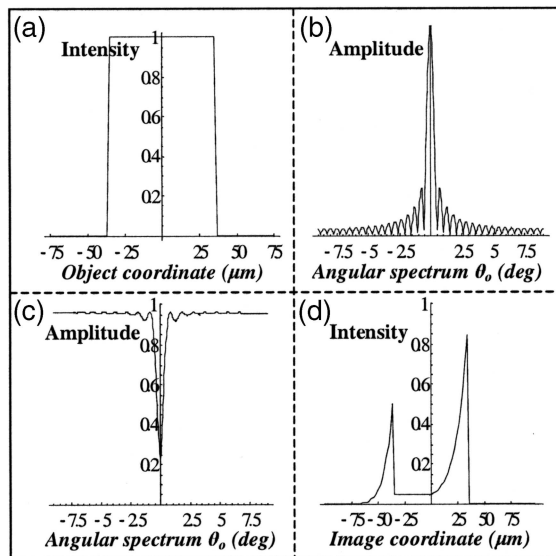


Fig. 3. Simulated results of the effect of the zero-order transfer function on an input image: (a) object, a slit of 70- $\mu\text{m}$  width; (b) frequency content of the object as a function of angle  $\theta_o$  (scaled with  $\lambda = 633$  nm); (c) zero-order transfer function of the photopolymer; (d) resultant filtered image.

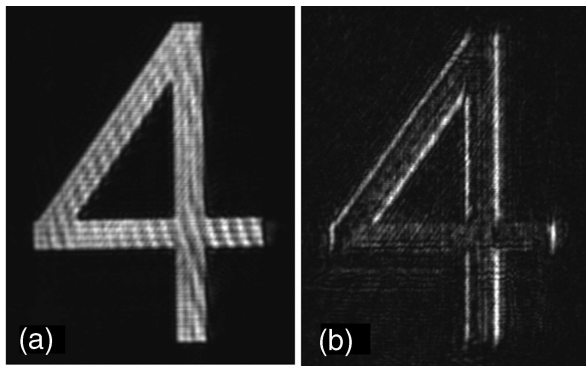


Fig. 4. Experimental images: (a) direct image with no grating, (b) zero-order filtered image.

in Fig. 2 when  $\psi = \theta_{\text{Bragg}}$ . We consider a one-dimensional object, i.e., the slit with width 70  $\mu\text{m}$  shown in Fig. 3(a). In Fig. 3(b) we plot the Fourier transform (modulus) of the object, scaled for  $\lambda_0 = 633$  nm (He-Ne laser). The frequency content is represented as a function of angle  $\theta_o$  (in degrees) for the plane-wave spectrum of the object. In Fig. 3(c) we show the modulus of the zero-order transfer function of the grating as a function of angle  $\theta_o$  (in degrees), with  $\psi = \theta_{\text{Bragg}}$ . We can see the sharp notch in the angular response. Finally, in Fig. 3(d) we plot the resultant filtered image produced by an imaging system with unit magnification. We obtain an edge-enhanced version of the input object. An interesting result is that the two edges are not equally enhanced. The simplified transfer function calculated by Davis and Nowack<sup>3</sup> predicts this result when  $\nu \neq \pi/2$ . In our case  $\nu \approx 1.34$  rad, which is less than  $\pi/2$ .

In Fig. 4 we show experimental results obtained by use of the setup of Fig. 1. First we calibrated the imaging resolution of the system, using the 1951 U.S.

Air Force test pattern as a negative (chrome-on-glass plate). The image resolution attained was better than 40.3 line pairs/mm, i.e., a period of 25  $\mu\text{m}$ . Next we imaged one of the objects in the test pattern. Figure 4(a) shows the direct image of the input object obtained by the imaging system when no grating is introduced. We observe a periodic pattern in the image that is the result of the interference produced by reflections at the interfaces (mainly at the chrome-on-glass plate). The width of the columns that compose the number 4 is approximately 70  $\mu\text{m}$ , like that of the object used in the simulations in Fig. 3. In Fig. 4(b) we show the zero-order image filtered by the photopolymer grating. We can clearly see the edge enhancement. It is remarkable that the horizontal edges are not enhanced; they are perpendicular to the grating periodicity. We can also see that the right-hand edge is slightly brighter than left-hand edge. This unequal edge enhancement was also predicted by the simulated results in Fig. 3. The image has not been digitally manipulated; thus the good quality of the edge-enhanced image indicates the low scattering noise generated by the PVA/acrylamide grating.

In conclusion, we have demonstrated the feasibility of a holographically edge-enhanced imaging system that uses a PVA/acrylamide photopolymer grating. Analytical expressions have been derived by use of Kogelnik's theory, which predicts the experimental results with good accuracy. We believe that image processing by Bragg diffraction offers an interesting application of holographic recording materials.

This research has been partially financed by the Ministerio de Ciencia y Tecnología, Spain, project MAT2000-1361-C04-04, and by the Generalitat Valenciana, Spain, project GV01-130. A. Márquez e-mail address is amarquez@dfists.ua.es.

## References

1. J. Xia, D. B. Dunn, T.-C. Poon, and P. P. Banerjee, *Opt. Commun.* **128**, 1 (1996).
2. D. Cao, P. P. Banerjee, and T.-C. Poon, *Appl. Opt.* **37**, 3007 (1998).
3. J. A. Davis and M. D. Nowak, *Appl. Opt.* **41**, 4835 (2002).
4. P. P. Banerjee, D. Cao, and T.-C. Poon, *Appl. Opt.* **37**, 7532 (1998).
5. P. Hariharan, *Optical Holography* (Cambridge U. Press, Cambridge, 1996).
6. J. Turunen and F. Wyrowski, eds., *Diffraction Optics for Industrial and Commercial Applications* (Springer-Verlag, Berlin, 1997).
7. S. K. Case, *Opt. Lett.* **4**, 286 (1979).
8. D. Peri and A. A. Friesem, *Opt. Lett.* **3**, 124 (1978).
9. H. J. Coufal, D. Psaltis, and B. T. Sincerbox, eds., *Holographic Data Storage* (Springer-Verlag, Berlin, 2000).
10. S. Blaya, L. Carretero, R. Mallavia, A. Fimia, R. F. Madrigal, M. Ulibarrena, and D. Levy, *Appl. Opt.* **37**, 7604 (1998).
11. S. Gallego, M. Ortuño, C. Neipp, C. García, A. Beléndez, and I. Pascual, *Opt. Commun.* **215**, 263 (2002).
12. H. Kogelnik, *Bell Syst. Tech. J.* **48**, 2909 (1969).